Available online at www.sciencedirect.com
ScienceDirect
Coordination Chemistry Reviews 252 (2008) 2346–2361
COORDINATION CHEMISTRY REVIEWS
www.elsevier.com/locate/ccr

Review

Ligand exchange and complex formation kinetics studied by NMR exemplified on *fac*-$[(CO)_3M(H_2O)]^+$ (M = Mn, Tc, Re)

Lothar Helm *

Ecole Polytechnique Fédérale de Lausanne, Institut des Sciences et Ingénierie Chimiques, BCH, CH-1015 Lausanne, Switzerland

Received 28 November 2007; accepted 7 January 2008
Available online 16 January 2008

Contents

Abstract

In this review ligand exchange and complex formation reactions on *fac*-$[(CO)_3M(H_2O)_3]^+$ (M = Mn, Tc, Re) and on *fac*-$[(CO)_2(NO)Re(H_2O)_3]^{2+}$ are presented. A variety of experimental NMR techniques are described and it is shown that sometimes combinations of techniques applied at variable temperature or variable pressure allowed to measure exchange rate constants and their activation parameters as well as thermodynamic parameters. Furthermore, the use of uncommon nuclei for NMR like ^{17}O or ^{99}Tc extends considerably the range of applications especially in aqueous solutions when ^1H NMR is often not very useful.

Tricarbonyl triaqua complexes of technetium(I) and rhenium(I) became important precursors for a variety of radiopharmaceuticals under development. It has been shown that the *fac*-$[(CO)_3M]$-unit is kinetically inert and that water molecules bound to it can be easily replaced. Reactivity of the Re^I complexes is one to two orders of magnitude slower than its Tc^I analogues. Furthermore, it shows a marked acidity dependence which has not been observed for Tc^I and Mn^I species.

Keywords: NMR; Ligand exchange reactions; Complex formation; Radiopharmacy; Carbonyl

1. Introduction

Since the beginning of the application of NMR in chemistry it has been used for quantitative determination of reaction rate constants [1–4]. The theory and reams of examples for exchange rate measurements by NMR can be found in books [5–8] and

* Tel.: +41 21 693 9876; fax: +41 21 693 9875.
E-mail address: lothar.helm@epfl.ch.

0010-8545/$ – see front matter © 2008 Elsevier B.V. All rights reserved.
doi:10.1016/j.ccr.2008.01.009

Table 1
Table of isotopes and nuclear moments of group 7 elements [25]

	Mn	Tc		Re			
	^{55}Mn	^{99}Tc	^{99m}Tc	^{185}Re	^{186}Re	^{187}Re	^{188}Re
Natural abundance	100%	–	–	37.40%	–	62.60%	–
Half-life	Stable	2.11×10^5 years	6.01 h	Stable	3.72 days	4.35×10^{10} years	17.0 h
Mode of decay	–	β (0.294 MeV)	IT (0.143 MeV)	–	β (1.069 MeV), ε (0.582 MeV)	(β, α)	β (2.12 MeV)
Nuclear spin	5/2	9/2	1/2	5/2	1	5/2	1
Electric quadrupole moment (10^{-28} m^2)	+0.32	−0.129		+2.2	+0.60	+2.08	+0.57

review articles [9–12]. The origin of success of NMR in the determination of reaction rate constants is certainly that it offers a variety of different experimental techniques based on relaxation studies, line shape analysis or simply recording spectra as a function time. Reactions with half-life of less than 10^{-9} s can be followed as well as reactions lasting for days or weeks [13]. A special feature of NMR is its possibility to study symmetric reactions like exchange reactions where starting materials and products are identical. Solvent exchange studies are prominent examples of such reactions. Nearly all water exchange rate constants on metal ions have been measured by NMR, mostly as a function of temperature but many of them also as a function of pressure to elucidate the mechanism of the reaction [14].

In this review, I would like to illustrate some less common NMR techniques using ^{1}H and other uncommon nuclei for NMR measurements. Our research group has been involved in the last decade in studies of solvent exchange and complex formation of technetium and rhenium compounds, work that has mainly been performed in collaboration with the groups of Roger Alberto (University of Zürich) and Roger Schibli (ETH Zürich).

The development of radiopharmaceuticals for diagnosis and treatment is an important research field of radiochemistry. Synthesis and characterization of radiolabelled compounds for imaging and therapy has strongly expanded over the last decade [15–19]. An important isotope for radioactive imaging agents is ^{99m}Tc and there is a strong interest in the development of new labelling techniques using this short-lived isotope. The use of the water-soluble tricarbonyl trihydrate technetium(I) cation, *fac*-$[(CO)_3Tc(H_2O)_3]^+$, as building block has allowed to synthesize a series of new, promising compounds [20–24]. Because the majority of compounds that have been labelled with ^{99m}Tc can also be labelled with ^{186}Re or ^{188}Re these complexes form couples that can be used for diagnosis (Tc) and therapy (Re) [20]. The three isotopes mentioned can be obtained from generator systems and have a half-life ranging from 6 h (^{99m}Tc) to 69 d (^{186}Re) (Table 1) [25,26]. Although no stable isotope of technetium exists its chemistry can be performed without severe radiation protection because the most stable isotope, ^{99}Tc, has a half-life of 2.11×10^5 years and is a weak β^- emitter without accompanying γ-radiation. This permits the handling of small amounts of ^{99}Tc in normal glassware like NMR tubes, since the β^- particles are shielded by even thin walls. Secondary X-rays become important only with larger amounts of ^{99}Tc [26]. Rhenium is found in nature as a mixture of two isotopes, ^{185}Re, which is stable, and ^{187}Re, which is a weak β^- emitter with a very long half-life of 4.35×10^{10} years (Table 1).

The technetium isotope used for imaging, ^{99m}Tc, is obtained from a ^{99}Mo generator [16] and has a relatively short life time. Therefore, the chemistry for preparation of the radiopharmaceuticals has to be fast, simple and lead to a high final purity. In a first step a stable but reactive precursor is prepared in aqueous solution from $[^{99m}TcO_4]^-$ [27]. From this precursor a complex has to be formed which has no structural or metal-based reactivity. Since its first synthesis *fac*-$[(CO)_3Tc(H_2O)]^+$ [28] became one of these precursors and a large number of substitution products have now been synthesized and structurally characterized [20,29–34]. Understanding reactivity and mechanisms of substitution of the three labile water molecules became an important issue especially in the context of synthesis of similar technetium and rhenium complexes. Manganese as the first member on the group 7 of the periodic table also forms tricarbonyl complexes in aqueous solution and it became evident to compare water exchange and complex formation of these three transition metal compounds.

2. Water exchange on *fac*-$[(CO)_3M(H_2O)]^+$ (M = Mn, Tc, Re)

A common issue of all tricarbonyl aqua complexes of group 7 elements is that the three water molecules are labile and the three carbonyl molecules are inert [20]. In reactions leading to radiopharmaceutical compounds the water molecules are replaced by one or more ligands forming stable products. Knowledge of the

Table 2
^{17}O and ^{13}C chemical shifts of triaqua tricarbonyl complexes in aqueous solution [36]

	δ (ppm)		
	$H_2{}^{17}O$	$C^{17}O$	^{13}CO
fac-$[(CO)_3Mn(H_2O)_3]^+$	−65	389	
fac-$[(CO)_3Tc(H_2O)_3]^+$	−52	352	210
fac-$[(CO)_3Re(H_2O)_3]^+$	−40	335	183
fac-$[(CO)_2(NO)Re(H_2O)_3]^{2+}$	−32[a]/−6[b]	389	188
fac-$[(CO)_3Ru(H_2O)_3]^+$[c]	−68	370	182

[a] *Trans* to CO.
[b] *Trans* to NO.
[c] From [37].

water exchange rate constant is therefore an important issue in the prediction of complex formation reactions.

Water exchange on metal ions and metal ion complexes can in general not be measured by ^{1}H NMR. The two main reasons for that are: (1) that H_2O binds via the oxygen atom to the metal and NMR properties like chemical shift and relaxation are most influenced on the close atom, and (2) very often and dependent on the acidity of the solution protons exchange is faster than exchange of the water molecule itself. A major drawback of this is that oxygen has only one isotope with a nuclear spin, oxygen-17, which has a very low natural abundance of 0.038% and a spin 5/2 and therefore a nuclear electric quadrupole moment leading to relatively broad NMR resonances [35]. In most cases work is performed using isotopic enriched samples.

In the case of slow exchange of water molecules, the ^{17}O chemical shift of H_2O in *fac*-$[(CO)_3M(H_2O)_3]^+$ is sufficiently large to allow direct observation of bound water (Table 2) [36]. The resonance of free H_2O is however several hundred to thousand times more intense, depending on the concentration of the complex in solution (Fig. 1). In many cases this intense signal has to be suppressed or at least strongly reduced. Solvent peak suppression is a common technique in ^{1}H NMR especially if NMR is coupled to HPLC or in aqueous solutions of bio-molecules. In ^{17}O NMR pulse sequences like Watergate or DANTE based techniques do not work because of the short T_1 of ~6 ms of bulk water. A short pulse sequence like the binomial 1-3-3-1 sequences proposed by Hore [38,39] works however well and can be used in many cases (Fig. 1, insert).

A chemical way to get rid of the bulk water signal is to add a relatively high concentration of a strong paramagnetic ion with fast water exchange like Mn^{2+}. Adding for example 0.1 mol kg^{-1} of Mn^{2+} broadens the bulk water peak to several tenth of kHz so that it becomes a broad hump and disappears in the baseline [40,41]. The broadening depends on the magnetic field used for the experiments as well as on temperature. Furthermore, this method can only be applied to acidic solutions because Mn^{2+} precipitates as hydroxide at higher pH.

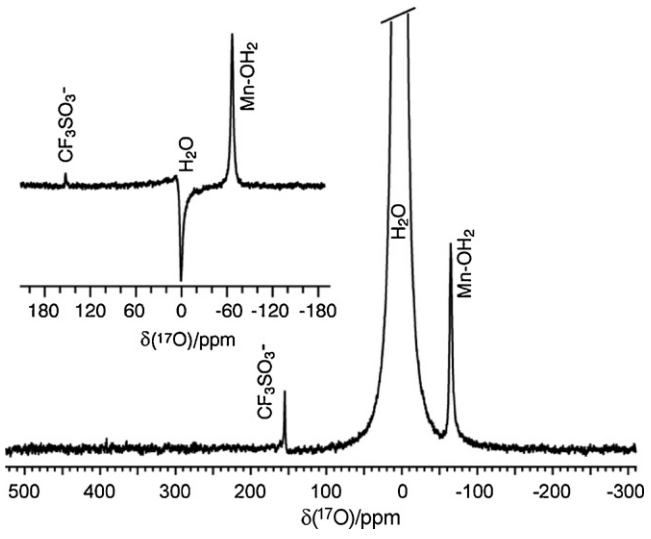

Fig. 1. ^{17}O NMR (54 MHz) spectra of a solution of 0.15 M *fac*-$[(CO)_3Mn(H_2O)_3]^+$ in 3.3 M aqueous CF_3SO_3H. ^{17}O enrichment 3.3%, T = 298 K. Spectrum in the upper left corner was recorded using the 1-3-3-1 pulse sequence. Note the remarkable intensity reduction of the bulk water signal compared to the main spectrum.

Water exchange rates on compounds of the type *fac*-$[(CO)_3M(H_2O)_3]^+$ vary over several orders of magnitude as a function of the transition metal, M. Therefore, different experimental approaches had to be used to measure the exchange rate constants, k_{ex}. Three examples of group 7 elements M = Mn^I, Tc^I and Re^I will be presented illustrating various NMR techniques.

2.1. Water exchange on *fac*-$[(CO)_3Mn(H_2O)_3]^+$

Water exchange on *fac*-$[(CO)_3Mn(H_2O)_3]^+$ is on one hand fast enough to produce a line broadening of the resonance of bound water in ^{17}O NMR and on the other hand slow enough to give two well resolved ^{17}O NMR signals corresponding to bound and free water (Fig. 1) [36]. The transverse relaxation of the ^{17}O nucleus in the bound state is obtained from the observed line-width at half height ($\Delta\nu_{1/2}$) by $1/T_{2obs} = \pi\,\Delta\nu_{1/2}$. Line broadening due to magnetic field inhomogeneity can in general be neglected. In the slow exchange limit $1/T_{2obs}$ is the sum of the exchange rate constant, k_{ex}, and the transverse relaxation rate of ^{17}O which is dominated by quadrupolar relaxation, $1/T_{2Q}$ (Eq. (1)):

$$\frac{1}{T_{2obs}} = \frac{1}{T_{2Q}} + k_{ex} \tag{1}$$

The inverse of k_{ex} is the mean residence time, τ_m, of water molecules in the first coordination sphere of *fac*-$[(CO)_3Mn(H_2O)_3]^+$. Therefore, k_{ex} is the exchange rate constant of a particular water molecule [42]. Increasing the temperature will increase k_{ex} and decrease the relaxation rate $1/T_{2obs}$. (Eqs. (2) and (3))

$$\frac{1}{T_{2Q}} = \frac{1}{T_{2Q}^{298}} \exp\left[\frac{E_Q}{R}\left(\frac{1}{T} - \frac{1}{298.15}\right)\right] \tag{2}$$

$$k_{ex} = \frac{k_B T}{h} \exp\left[\frac{\Delta S^{\ddagger}}{R} - \frac{\Delta H^{\ddagger}}{RT}\right] = \frac{T k_{ex}^{343}}{343.15} \exp\left[-\frac{\Delta H^{\ddagger}}{RT}\left(\frac{1}{T} - \frac{1}{343.15}\right)\right] \tag{3}$$

At high temperatures the small signal of bound water becomes broad and overlaps considerably with the huge signal of free water. Furthermore, at $T > 323$ K and increasing pH the compound decomposes slowly forming strongly paramagnetic Mn^{2+} which itself broadens the free water signal strongly. This decomposition has however no influence on the line-width of bound water and therefore on the measurement of k_{obs}. To be able to measure $1/T_{2obs}$ accurately the free water signal has been suppressed using the 1-3-3-1 pulse sequence [38,39]. If the complex undergoes hydrolysis, the water exchange will also take place on the hydrolyzed species $[(CO)_3Mn(H_2O)_2(OH)]$

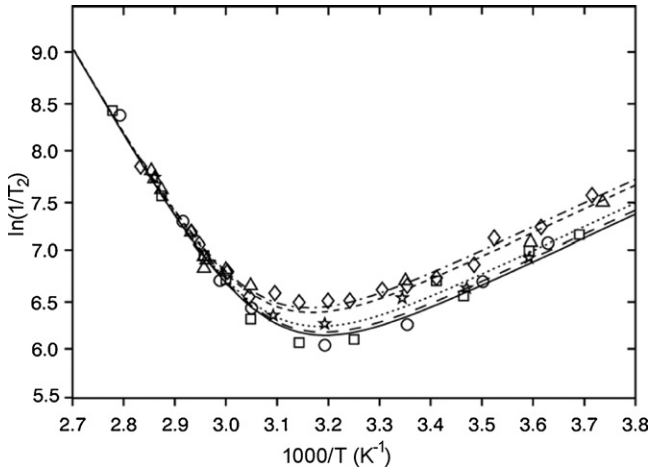

Fig. 2. Temperature dependence of the transverse relaxation rate ($1/T_2$) of the ^{17}O NMR signal of bound water in *fac*-$[(CO)_3Mn(H_2O)_3]^+$ in five different acidity domains ((◯—) $[H^+] = 0.4$ M; (□– –) $[H^+] = (1.2–1.4) \times 10^{-2}$ M; (◇---) $[H^+] = (2–3) \times 10^{-4}$ M; (△- -) $[H^+] = (3–6) \times 10^{-5}$ M; (☆···) $[H^+] = (0.5–1) \times 10^{-6}$ M; lines represent best fit.

and the observed rate constant is given by Eq. (4) [43]:

$$k_{obs} = \frac{k_{ex} + k_2}{[H^+]} = \frac{k_{ex} + k_{OH} K_a}{[H^+]} \quad (4)$$

where k_{ex} is the water exchange rate on *fac*-$[(CO)_3Mn(H_2O)_3]^+$ and k_2 is the rate on the hydrolyzed compound. At high temperatures where k_{obs} is dominating experimental $1/T_{2obs}$ values are independent on acidity over a range of pH 1–6 in the case of manganese(I) (Fig. 2). The exchange pathway via the hydrolyzed species can therefore be neglected in the data analysis. However, the quadrupolar relaxation increases with pH and therefore individual $1/T_{2Q}^{298}$ (Eq. (2)) have to be used in the data analysis. This variation is most probably due to changes in the composition and viscosity of the solutions because the activation energy E_Q (20.5 ± 1 kJ mol^{-1}) is not affected. The water exchange rate k_{ex} is best defined at $1000/T \sim 2.9$ K^{-1}: $k_{ex}^{343} = 1220 \pm 40$ s^{-1} where the measured $1/T_{2obs}$ is largely dominated by k_{obs} [43].

2.2. Water exchange on fac-[(CO)$_3$Tc(H$_2$O)$_3$]$^+$

Water exchange on *fac*-$[(CO)_3Tc(H_2O)_3]^+$ is much more difficult to measure. The exchange rate is too slow to produce a measurable line broadening. At low temperature $T = 277$ K the exchange rate is however slow enough to be measured by isotopic exchange. If water enriched in $H_2{}^{17}O$ is rapidly injected [44] into a solution of *fac*-$[(CO)_3Tc(H_2O)_3]^+$ in natural abundance water the enrichment of bound water with ^{17}O can be followed by NMR (Fig. 3) [36]. To get a reasonable signal of bound $H_2{}^{17}O$ in a short time (2.9 s) a relatively high enrichment in the final solution has to be achieved. Furthermore, because the experiment is performed at low temperature both components to be mixed have to be prethermostated using a special device [44]. The integrals of the peaks can be fitted to Eq. (5). χ_∞ is in this case the mole fraction of coordinated $H_2{}^{17}O$ at t_∞ and $I(t)$ and I_∞ denote the signal integrals of metal bound H_2O at t and at t_∞.

$$I(t) = I_\infty \left(1 - \exp\left(\frac{k_{ex} t}{1 - x_\infty}\right)\right) \quad (5)$$

The exchange rate constant fitted is $k_{ex}^{277} = 0.044 \pm 0.002$ s^{-1} corresponding to a half-life of 16.8 s. Exchange rates have been measured at pH 1.4 and 4.3 and were found independent on acidity.

Measuring k_{ex} for *fac*-$[(CO)_3Tc(H_2O)_3]^+$ at higher temperatures is very difficult: the rates are too fast for isotopic enrichment experiments. The line shape of $H_2{}^{17}O$ bound to Tc^I is in principle a decuplet due to coupling to ^{99}Tc ($I = 9/2$). Experimentally observed is an ^{17}O NMR line shape which changes from a large bump at higher temperatures to an "M" shaped signal and an almost rectangular shape at lower temperature (Fig. 4) [43]. In the case of coupling to a nucleus with an electric quadrupole moment ($I > 1/2$) the shape of the multiplet is influenced by the relaxation of that nuclear spin due to quadrupolar relaxation [45]. If the nuclear quadrupole moment is large as for example for ^{55}Mn and $^{185/187}$Re quadrupolar relaxation of the metal nuclear spin is fast. The multiplet of the observed ^{17}O spin collapses completely and a single Lorentzian line shape is observed despite the coupling. ^{99}Tc has the smallest quadrupole moment of the metals studied which together with the relatively symmetric environment in *fac*-$[(CO)_3Tc(H_2O)_3]^+$ leads to a relatively slow relaxation of ^{99}Tc and therefore coupling can be observed. Besides relaxation of the metal nuclear spin the residence time in the bound state of the observed nucleus, τ_m, also influences the observed line shape. Because this residence time is simply the inverse of the exchange rate constant, $\tau_m = 1/k_{ex}$ the line shape of the ^{17}O signals of bound water can be used to determine k_{ex}. Parameters influencing the line shape of the observed ^{17}O resonance (Fig. 4) are the longitudinal relaxation of ^{99}Tc ($1/T_{1Q}$), the coupling constant between ^{17}O and ^{99}Tc, $^1J_{^{17}O,^{99}Tc}$, the ^{17}O quadrupolar relaxation of bound water molecules, $1/T_{2Q}$, and the exchange rate constant, k_{ex}. Using $^1J_{^{17}O,^{99}Tc} = 80$ Hz (from ^{99}Tc NMR [43]) and

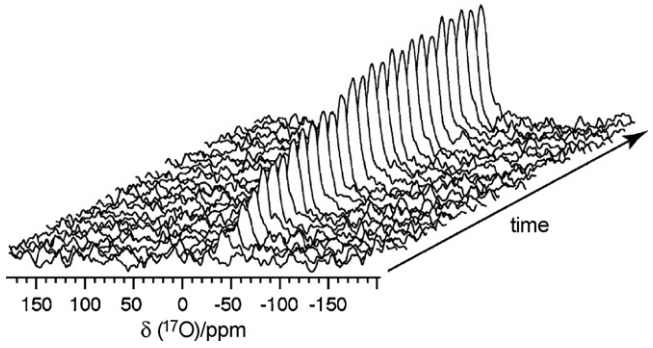

Fig. 3. ^{17}O NMR spectra (54 MHz) of a solution of *fac*-$[(CO)_3Tc(H_2O)_3]^+$ after injection of ^{17}O enriched water showing the increase of the signal of bound water in *fac*-$[(CO)_3Tc(H_2O)_3]^+$. Time increment between two spectra is 2.9 s. Mn^{2+} was added to remove the signal of bulk water. [Tc] = 0.054 M, 4.6% ^{17}O, $[H^+] = 4.0 \times 10^{-5}$ M (PIPBS buffer), $I = 1$ M ($NaClO_4$), $[Mn^{2+}] = 0.2$ M, $T = 277$ K.

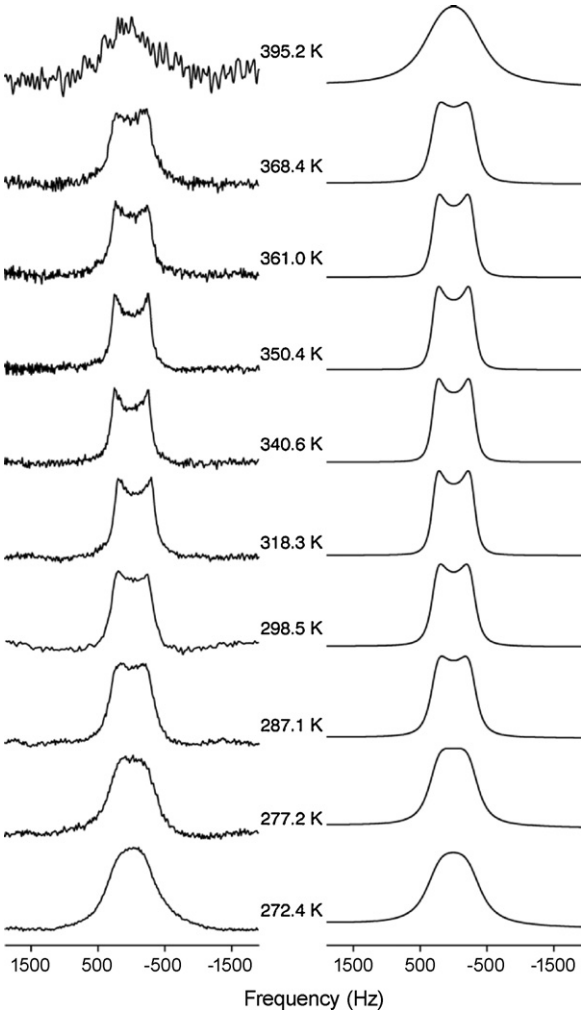

Fig. 4. Calculated (left) and experimental (right) ^{17}O NMR spectra (54 MHz) showing the signal of bound water in *fac*-$[(CO)_3Tc(H_2O)_3]^+$ as a function of temperature. Mn^{2+} was added to remove the signal of bulk water.

a phenomenological description of $1/T_{1Q}$ [36] the transverse relaxation rate of ^{17}O, $1/T_{2obs} = 1/T_{2Q} + k_{ex}$, has been calculated for each temperature by fitting theoretical line shapes to experimental spectra (Figs. 4 and 5). The $1/T_{2obs}$ determined are the sum of the ^{17}O quadrupolar relaxation (dominant at low temperature) and the exchange rate constant k_{ex} (dominant at high temperature). A simultaneous fit of the ten $1/T_{2obs}$-values from line shape analysis together with the unique value of k_{ex} ($T = 277$ K) from isotopic enrichment experiment (Eqs. (1)–(3)) allows a precise determination of k_{ex} ($k_{ex}^{298} = 0.49 \pm 0.05\ s^{-1}$) and its activation parameters $\Delta H^{\ddagger}$ (78.3 ± 1 kJ mol^{-1}) and $\Delta S^{\ddagger}$ ($+11.7 \pm 3$ J K^{-1} mol^{-1}) (Fig. 5). This example nicely illustrates that combining different NMR techniques sometimes allows extending the temperature range accessible experimentally for measuring k_{ex}.

2.3. Water exchange on *fac*-$[(CO)_3Re(H_2O)_3]^+$

Water exchange on *fac*-$[(CO)_3Re(H_2O)_3]^+$ is much slower than on its technetium analogue and therefore isotopic enrichment experiments allow to measure k_{ex} not only at

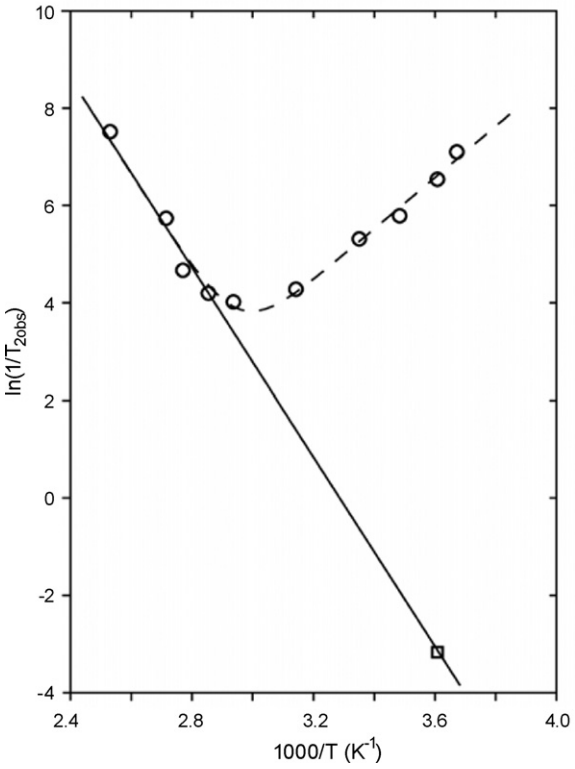

Fig. 5. Transverse relaxation rate ($1/T_{2obs}$) temperature dependence of the ^{17}O NMR signal of bound water in *fac*-$[(CO)_3Tc(H_2O)_3]^+$. The dashed line represents the best fit of Eq. (2) to $\ln(1/T_{2obs})$ experimental points (◯). The solid line corresponds to Eq. (3) including the $\ln(k_{ex}^{277})$ value (□).

low temperature (Fig. 6) [46]. These experiments are often very time-consuming and expensive because considerable amounts of enriched $H_2{}^{17}O$ (10% enrichment) have to be used. Exchange rates measured at variable temperature are shown in Fig. 7 and the corresponding activation parameters are $\Delta H^{\ddagger} = 90 \pm 3$ kJ mol^{-1} and $\Delta S^{\ddagger} = +14 \pm 10$ J K^{-1} mol^{-1} ($k_{obs}^{298} = (5.4 \pm 0.3) \times 10^{-3}\ s^{-1}$). The larger errors on the fitted parameters reflect the smaller temperature range available if compared for example to those determined for the Tc analogue.

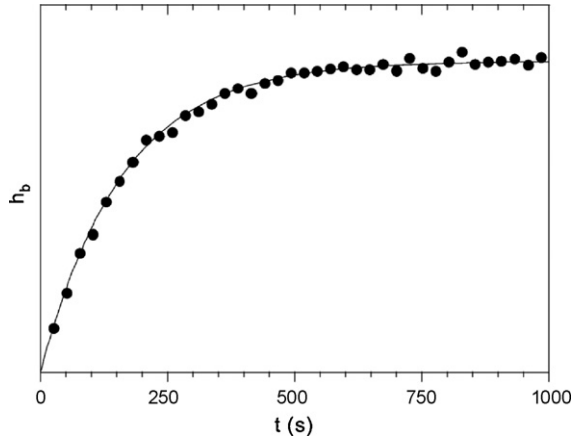

Fig. 6. Increase as a function of time of ^{17}O NMR signal height h_b (arbitrary units) of bound water in *fac*-$[(CO)_3Re(H_2O)_3]^+$ (0.1 M CF_3SO_3H; $I = 1$ M), at $T = 298$ K; experimental values (●), fit according to Eq. (5) (—).

Table 3
Selected kinetic data and mechanisms of water exchange for aqua complexes of Cr(0), W(0), Mn(I), Tc(I), Re(I), Ru(II),

	k_{ex}^{298} (s^{-1})	$\Delta H^{\ddagger}$ (kJ mol^{-1})	$\Delta S^{\ddagger}$ (J K^{-1} mol^{-1})	$\Delta V^{\ddagger}$ (cm^3 mol^{-1})	Mechanism	pK_a	Ref.
$[(CO)_3Cr(H_2O)_3]$	11×10^4	50	+20			<8	[51]
$[(CO)_3W(H_2O)_3]$	31	58	−22			<4.5	[51]
$[(CO)_3Mn(H_2O)_3]^+$	23	72.5	+24.4	+7.1	I_d	9–10	[43]
$[(CO)_3Tc(H_2O)_3]^+$	0.49	78.3	+11.7	+3.8	I_d		[43]
$[(CO)_3Re(H_2O)_3]^+$	6.3×10^{-4}	90.3	+14.5		I_d	7.5	[46]
$[(CO)_3Re(OH)(H_2O)_2]$	27						[46]
$[(CO)_3Ru(H_2O)_3]^{2+}$	10^{-4}–10^{-3}					−0.14	[37]
$[(CO)_3Ru(OH)(H_2O)_3]^+$	5.3×10^{-2}						[37]

In the case of water exchange on the Re^I compound a marked acidity dependence of k_{obs} has been observed. It is therefore likely that in this case not only *fac*-$[(CO)_3Re(H_2O)_3]^+$ but also *fac*-$[(CO)_3Re(OH)(H_2O)_2]$ contributes to the observed exchange rate in a proportion determined by the acid dissociation constant K_a (Eq. (6) and Table 3):

$$K_a = \frac{[(CO)_2Re(OH)(H_2O)_2]}{[(CO)_2Re((H_2O)_3^+][H^+]} \quad (6)$$

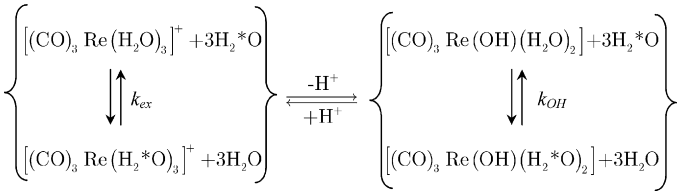

(7)

The observed exchange rate constant k_{obs} is given by Eq. (4) and a linear relation of k_{obs} versus $[H^+]^{-1}$ is expected. The experimental data confirm this linear dependence (Fig. 8) and k_{ex} and k_{OH} can be determined if K_a is known. Taking $\log K_a = -7.5$ from literature [47] $k_{ex} = (6.3 \pm 0.1) \times 10^{-3}\ s^{-1}$ and $k_{OH} = 27 \pm 1\ s^{-1}$ are obtained. These results show that at pH < 2.5 exchange proceeds mainly on *fac*-$[(CO)_3Re(H_2O)_3]^+$. At pH > 4 the contribution of *fac*-$[(CO)_3Re(OH)(H_2O)_2]$ becomes predominant for water exchange on tricarbonyl Re^I.

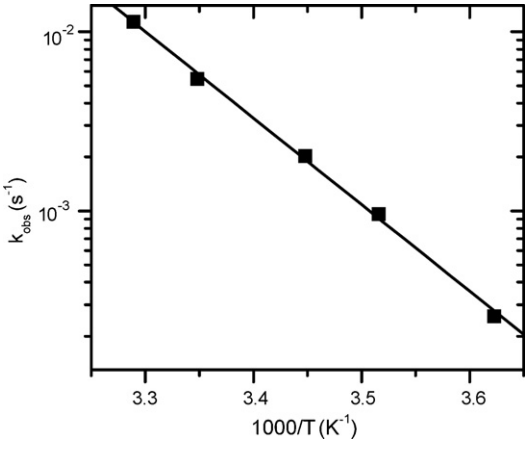

Fig. 7. Temperature dependence of k_{obs} for water exchange on *fac*-$[(CO)_3Re(H_2O)_3]^+$ (■) (0.1 M ClO_4^-, I = 0.25 M). The solid line corresponds to a fit with Eq. (3).

2.4. Water exchange on *fac*-$[(CO)_3M(H_2O)]^+$-comparisons

Comparing water exchange rate constants for tricarbonyl aqua ions of group 7 metals shows that k_{ex} is strongly decreasing when going down the group. Including the data available for the Cr, W and Ru homologues, the same trend is observed in group 6 (Table 3). In a row going from left to right the decrease of the water exchange rate is paralleled by a charge increase of these isoelectronic (t_{2g}^6) complexes. A similar behaviour has been reported for $[Ru(H_2O)_6]^{2+}$ and $[Rh(H_2O)_6]^{3+}$ aqua ions [48,49], where the increase in bond strength leads even to a change in the water exchange mechanism from I_d to I_a [50]. The electrostatic interaction is influencing the metal water bond strength which is also clearly visible in the increased activation enthalpies, $\Delta H^{\ddagger}$, for the water exchange (Table 3) and certainly also contributes to the slower water exchange rates on *fac*-$[(CO)_2(NO)Re(H_2O)_3]^{2+}$ (see below).

3. CO exchange on *fac*-$[(CO)_3Tc(H_2O)_3]^+$

Even if the carbonyls in *fac*-$[(CO)_3M(H_2O)_3]^+$ are rather inert a slow exchange with free CO in solution can be observed. To measure the exchange rate constant, k_{CO}, of CO on *fac*-$[(CO)_3Tc(H_2O)_3]^+$ a solution was pressurized with 4.4 MPa of ^{13}CO in a 10 mm NMR sapphire tube [52,53]. The CO exchange

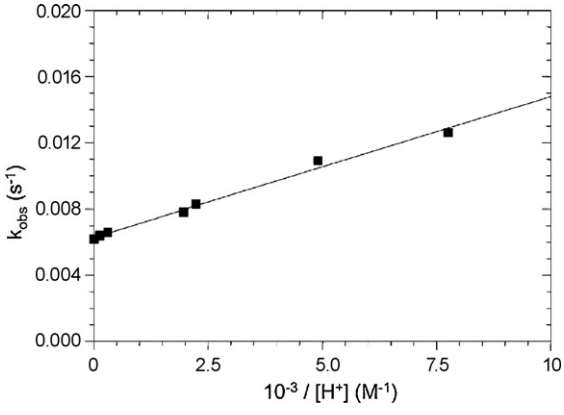

Fig. 8. Acidity dependence of the water exchange rate on tricarbonyl Re^I at T = 298 K; rate constants k_{obs} (■) and best fit (—); I = 1.0 M (Na CF_3SO_3).

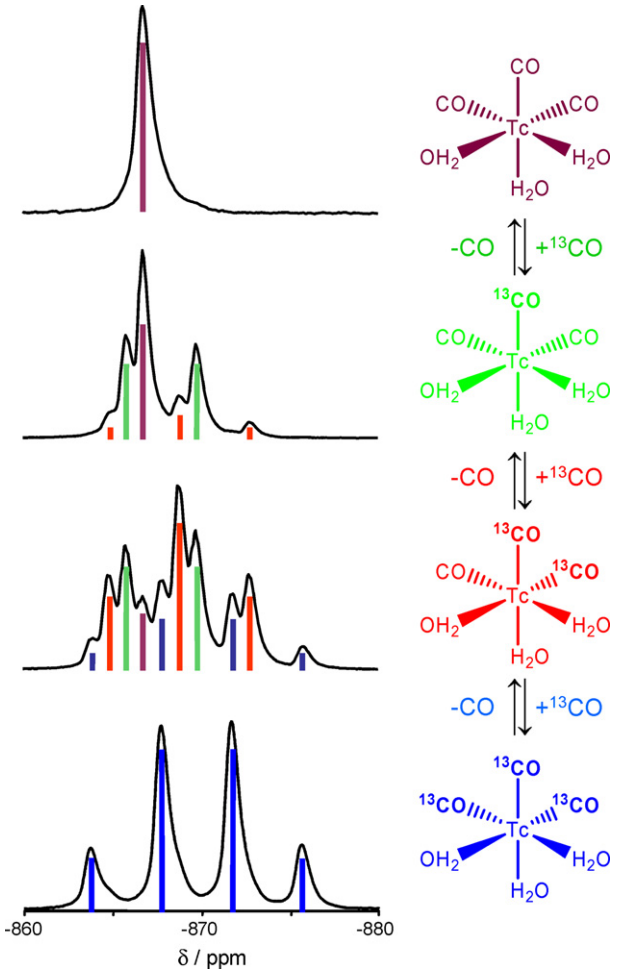

Fig. 9. Time evolution of ^{99}Tc NMR spectra recorded at 277 K of an aqueous solution of *fac*-$[(CO)_3Tc(H_2O)_3]^+$ under ^{13}CO (~5 MPa). The spectra were recorded (from top to bottom) after 2 min, 4 h, 35 h, 10 d.

was monitored by ^{99}Tc NMR (Fig. 9) [54]. Substitution of the NMR coupling silent ^{12}CO by one, two or three NMR coupling active ^{13}CO led to the successive appearance and disappearance of various multiplets. In addition, each substitution of one ^{12}CO by one ^{13}CO causes an isotopic shift of $\Delta\delta = -1.05$ ppm per carbon mass unit.

The mole fractions of the different isotopomers as a function of time are obtained by fitting sums of singlets, doublets, triplets and quartets to the experimental spectra. Using a mathematical description developed for complex formation [55] the second order rate constant k_{CO} can be obtained from a simultaneous fit of all mole fractions. Results at two temperatures measured by either pressurizing *fac*-$[(CO)_3Tc(H_2O)_3]^+$ with ^{13}CO or *fac*-$[(^{13}CO)_3Tc(H_2O)_3]^+$ with ^{12}CO are shown in Fig. 10 [54]. The fitted rate constants are $k_{CO} = (10.0 \pm 0.2) \times 10^{-4}\ s^{-1}\ M^{-1}$ ($T = 310$ K) and $k_{CO} = (0.82 \pm 0.01) \times 10^{-4}\ s^{-1}\ M^{-1}$ ($T = 277$ K). A comparison with water exchange rates shows that exchange of carbonyls is two to three orders of magnitude slower than the exchange of water molecules confirming the kinetic inertness of the $[(CO)_3Tc]$ moiety.

4. Replacement of H_2O by CO, formation of $Tc(CO)_6$

Ten years ago Ziegler published DFT calculated ^{13}C chemical shifts of a series of hexacarbonyls, including $[Tc(CO)_6]^+$ which had not been synthesized at that time [56]. In 2000, Aebischer et al. could show by ^{13}C and ^{99}Tc NMR that the hexacarbonyl of Tc^I is formed in aqueous solution under CO pressure [54]. A solution of *fac*-$[(CO)_3Tc(H_2O)_3]^+$ has been kept in a sapphire NMR tube under ~5 MPa of ^{13}CO for about 3 weeks at room temperature. The ^{99}Tc NMR spectrum recorded after that time showed besides the quartet at −867 ppm due to *fac*-$[(^{13}CO)_3Tc(H_2O)]^+$ three signals at lower frequencies (Fig. 11). The septet at $\delta = -1961$ ppm clearly shows that $[Tc(^{13}CO)_6]^+$ is present in the sample. The additional peaks at $\delta = -1050$ and −1418 ppm are much broader and do not show any multiplet structure. From the assumption that each CO replacing a water molecule shifts the ^{99}Tc to lower frequency the signals were attributed to $[(CO)_4Tc(H_2O)_2]^+$ and $[(CO)_5Tc(H_2O)]^+$, respectively [54]. The broadening of the NMR signals of the quadrupolar ^{99}Tc is probably due to the reduction of symmetry on the Tc-centre, increasing therefore quadrupolar relaxation of ^{99}Tc [57].

The ^{13}C spectrum of the same sample exhibits after releasing ^{13}CO pressure two decuplets at $\delta = 209.7$ and 190.2 ppm (Fig. 12). The $^1J_{^{17}O,^{99}Tc}$ coupling constants of the two are identical to those of the quartet (354 Hz) and the septet (261 Hz) measured by ^{99}Tc NMR allowing their assignment to $[(^{13}CO)_3Tc(H_2O)_2]^+$ and $[Tc(^{13}CO)_6]^+$, respectively. The ^{13}C chemical shift of $[Tc(^{13}CO)_6]^+$ is in excellent agreement with the value of 193.1 ppm calculated by Ziegler. The hexacarbonyl complex is relatively stable in aqueous solution at acidic pH and release of CO from the molecule is slow. Upon release of CO pressure the ^{99}Tc peaks attributed to $[(CO)_4Tc(H_2O)_2]^+$ and $[(CO)_5Tc(H_2O)]^+$ disappear within 1 h whereas the signal due to $[Tc(^{13}CO)_6]^+$ disappears slowly within 2 days at room temperature [54]. Alberto [58] suggests that once one CO is replaced by a water molecule two other CO's are cleaved rapidly following Fig. 13.

5. Oxygen exchange on *fac*-$[(CO)_3Mn(H_2O)_3]^+$

If a tricarbonyl complex is dissolved in water the carbonyl oxygen exchange very slowly with water oxygen as it has been observed on hexacarbonyl ions, for example [59,60]. A quantitative study using ^{17}O isotopic exchange has been reported for *fac*-$[(CO)_3Mn(H_2O)_3]^+$ [43,61]. To be able to follow the increase with time of the $C^{17}O$ signal after dissolution of the un-enriched complex in ^{17}O enriched water the huge signal of bulk water had to be depressed (Fig. 14) [38,39]. Manganese(I) in *fac*-$[(CO)_3Mn(H_2O)_3]^+$ is slowly oxidized and the complex decomposes forming Mn^{2+} aqua ions. As already explained above, water exchange on these very paramagnetic ions is fast and the peak of bulk water broadens more and more on consecutive spectra as Mn^{2+} concentration is increasing. However, a quantitative analysis of ^{17}O exchange on CO is still possible due to the peak of water bound to Mn^I serving as reference for integration of the peaks. The increase in time of the relative signal

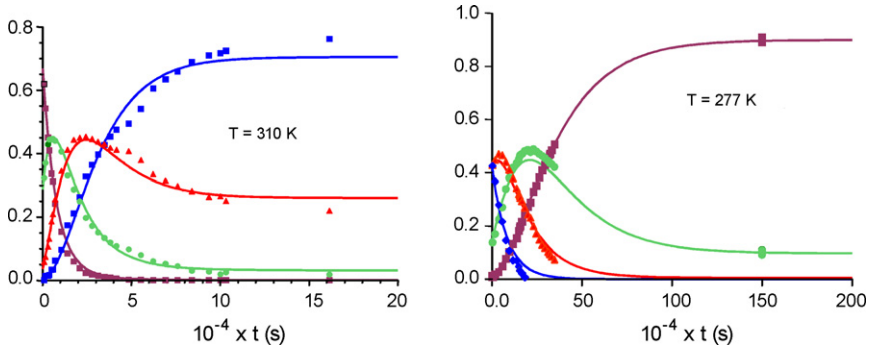

Fig. 10. Evolution of the mole fractions of the isotopomers of *fac*-$[(^{12}CO)_3Tc(H_2O)_3]^+$ under 4.4 MPa of ^{13}CO (left) and of *fac*-$[(^{13}CO)_3Tc(H_2O)_3]^+$ under 4.4 MPa of ^{12}CO (right): *fac*-$[(^{12}CO)_3Tc(H_2O)_3]^+$ brown; *fac*-$[(^{12}CO)_2(^{13}CO)Tc(H_2O)_3]^+$ green; *fac*-$[(^{12}CO)(^{13}CO)_2Tc(H_2O)_3]^+$ red; *fac*-$[(^{13}CO)_3Tc(H_2O)_3]^+$ blue.(For interpretation of the references to colour in this figure legend, the reader is referred to the web version of the article.)

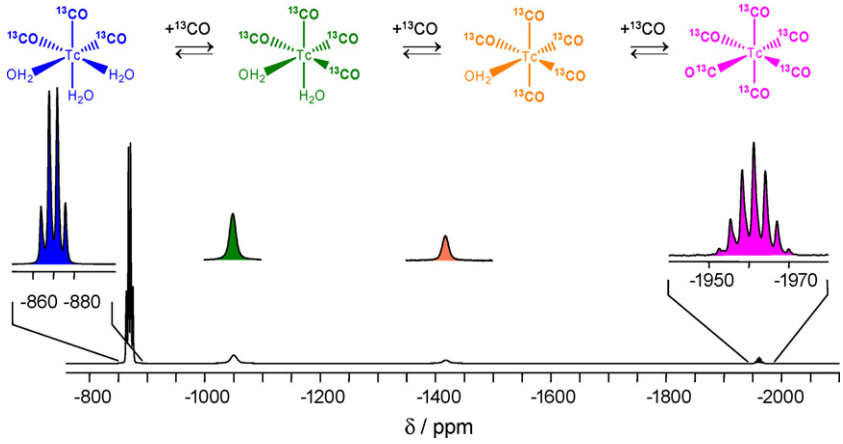

Fig. 11. ^{99}Tc NMR spectrum recorded at 310 K of a solution kept 20 days under ^{13}CO (~5 MPa) at room temperature (chemical shift reference: TcO_4^-).

intensity $I(t)/I_\infty$ is given by Eq. (5). The exchange rate constant for CO-oxygen is k_{C^*O}, x_∞ is the mole fraction of bound oxygen (<1%), and I_∞, the integral at equilibrium, is equal to the integral of bound water. Due to the slow oxidation of Mn^I the exchange reaction could only be followed for about 19 h which is less than one half-life for the exchange reaction (Fig. 15). However, a relatively precise determination of k_{C^*O}, was possible because I_∞ is known from the ^{17}O signal of bound water. The exchange rate determined at 338 K is $4.3 \times 10^{-6}\ s^{-1}$ corresponding to a half-life of ~45 h [43] and the reaction is assumed to proceed via the formation of a metallacarboxylic acid [61].

6. Complex formation reactions on *fac*-$[(CO)_3M(H_2O)_3]^+$

Tricarbonyl complexes of Tc^I and Re^I are interesting precursors for radiopharmaceuticals because the three water ligands

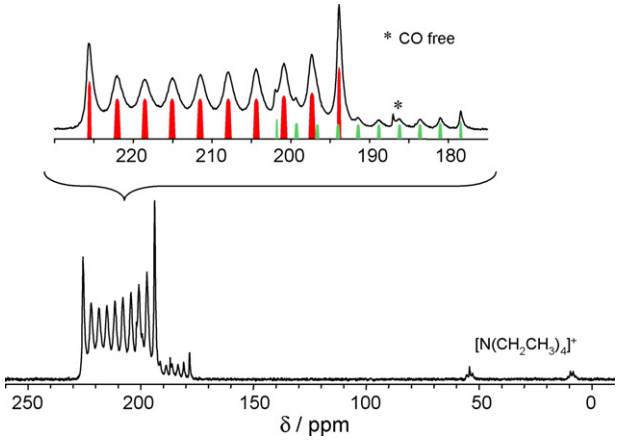

Fig. 12. ^{13}C NMR spectrum recorded at 335 K of a solution kept 20 days under ^{13}CO (~5 MPa) after releasing CO pressure.

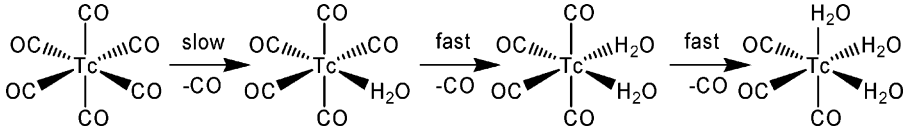

Fig. 13. Formation of *fac*-$[(CO)_3Tc(H_2O)_3]^+$ from $[Tc(CO)_6]^+$.

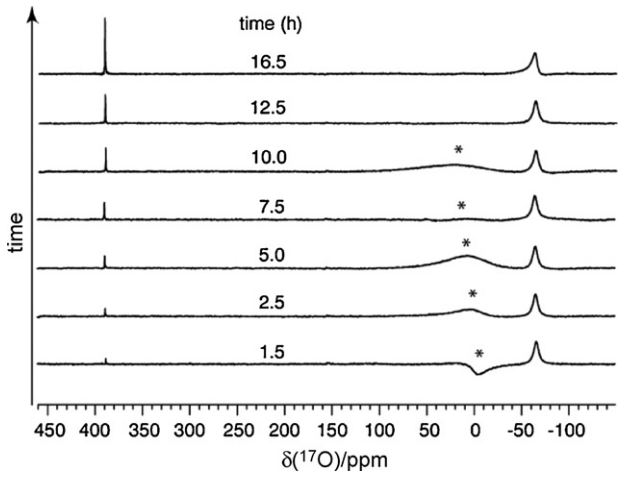

Fig. 14. ^{17}O NMR spectra of an ^{17}O enriched solution of *fac*-$[(CO)_3Mn(H_2O)_3]^+$ heated to 338 K, showing the progressive increase of the signal at 389 ppm due to ^{17}O enrichment of the carbonyl ligand. Coordinated water is observed at −65 ppm. Bulk water (*) has been suppressed, by a 1-3-3-1 pulse sequence, and broadened after some time by the Mn^{2+} resulting from the decomposition of some complex.

can readily be replaced by incoming ligands and a large number of compounds have been synthesized and characterized [18,20,21,23,24,29]. Both M^I centres bind a variety of ligand atoms like nitrogen, phosphorous, oxygen and sulfur. Because the half-life of the radioisotopes used in radiopharmaceuticals are in general short, the preparation of the complexes must be fast and complete. Therefore, knowledge of kinetics and mechanism of complex formation of *fac*-$[(CO)_3M(H_2O)_3]^+$ with a diversity of ligands with different binding atoms is important (Fig. 16).

Monodentate ligands like acetonitrile or DMS can replace successively all three water molecules as can be shown by ^1H NMR (Fig. 17) [36,46]. After mixing aqueous solutions of *fac*-$[(CO)_3Re(H_2O)_3]^+$ and DMS signals due to mono, bi, and tri complexes (*fac*-$[(CO)_3Re(DMS)(H_2O)_2]^+$: 2.65 ppm, *fac*-$[(CO)_3Re(DMS)_2(H_2O)]^+$: 2.74 ppm; *fac*-$[(CO)_3Re(DMS)_3]^+$:

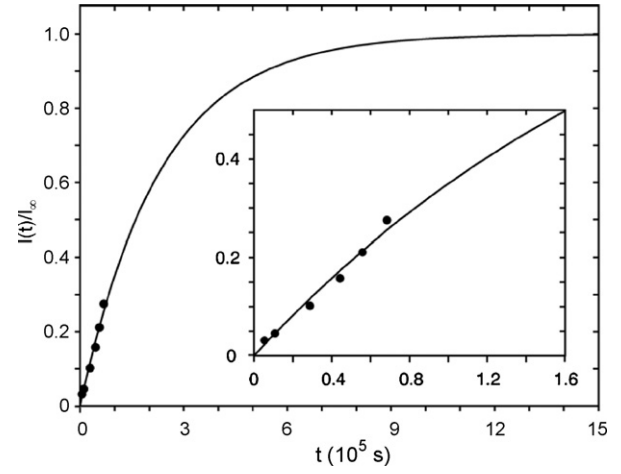

Fig. 15. Evolution of the integral of the CO peak in ^{17}O NMR of an ^{17}O enriched solution of *fac*-$[(CO)_3Mn(H_2O)_3]^+$ heated to 338 K; the solid line represents the best fit.

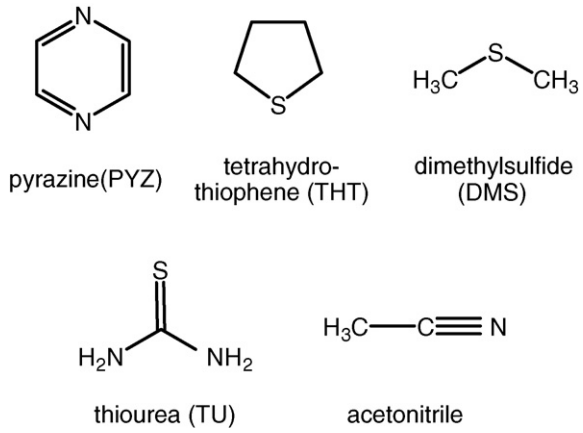

Fig. 16. Ligands used for studies of complex formation kinetics on *fac*-$[(CO)_3M(H_2O)_3]^+$.

2.81 ppm) appear after several hours. Once equilibrium is established the thermodynamic equilibrium constants of successive complex formation, K_1, K_2 and K_3, can be determined from integration of the NMR signals. As an example, for the complexation of the Re^I compound with DMS the following constants have been determined ($T = 298$ K): $8.3 \pm 0.1\ M^{-1}$ (K_1), $46.8 \pm 0.8\ M^{-1}$ (K_2), $52 \pm 6\ M^{-1}$ (K_3) [62]. In this example, where ^1H resonances are not overlapping and the kinetics is slow, all rate constants for formation and dissociation can be determined. Three formation rate constants $k_{f,i}$ ($i = 1$–3) and the equilibrium constants K_i characterize the three reactions (Eq. (8)).

$$[(CO)_3M(H_2O)_3]^+ + L \underset{k_{r,1}}{\overset{k_{f,1}}{\rightleftarrows}} [(CO)_3M(L)(H_2O)_2]^+ + H_2O; \quad K_1 = \frac{k_{f,1}}{k_{r,1}}$$
$$[(CO)_3M(L)(H_2O)_2]^+ + L \underset{k_{r,2}}{\overset{k_{f,2}}{\rightleftarrows}} [(CO)_3M(L)_2(H_2O)]^+ + H_2O; \quad K_2 = \frac{k_{f,2}}{k_{r,2}}$$
$$[(CO)_3M(L)_2(H_2O)]^+ + L \underset{k_{r,3}}{\overset{k_{f,3}}{\rightleftarrows}} [(CO)_3M(L)_3]^+ + H_2O; \quad K_3 = \frac{k_{f,3}}{k_{r,3}} \tag{8}$$

Assuming second-order kinetics, the variation of the concentrations of all observed species can be calculated as functions

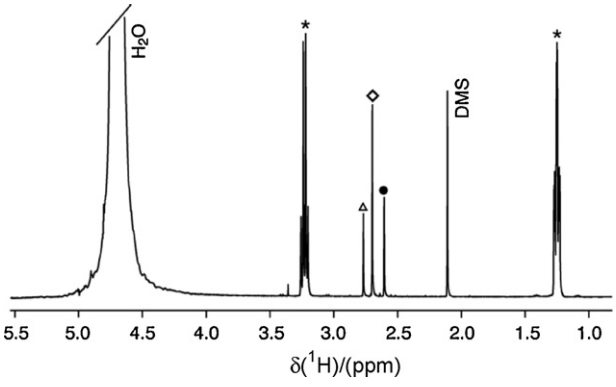

Fig. 17. ^1H NMR (400 MHz) spectrum of a solution containing initially *fac*-$[(CO)_3Re(H_2O)_3]^+$ 0.05 M and DMS 0.09 M, recorded at 298 K 32 h after addition of DMS. *fac*-$[(CO)_3Re(DMS)(H_2O)_2]^+$ (●), *fac*-$[(CO)_3Re(DMS)_2(H_2O)]^+$ (◊) and *fac*-$[(CO)_3Re(DMS)_3]^+$ (△), $(C_2H_5)_4N^+$ (☆).

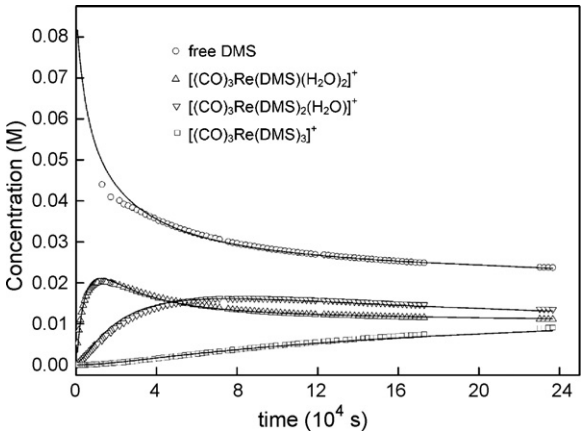

Fig. 18. Concentrations of free DMS and of the mono, bi, and tri complexes as a function of time (T = 298 K). Initial composition: *fac*-$[(CO)_3Re(OH_2)_3]^+$ 0.05 M, DMS 0.09 M, 0.1 M CF_3SO_3H.

of $k_{f,i}$ and K_i (see Supplementary Material of [46]; Fig. 18). A simultaneous fit of the time dependence of all concentrations obtained from peak integrals leads to $k_{f,1}$ ($k_{r,1}$): $(1.18 \pm 0.06) \times 10^{-3}$ $((0.142 \pm 0.008) \times 10^{-3})\,M^{-1}\,s^{-1}$, $k_{f,2}$ ($k_{r,2}$): $(0.76 \pm 0.02) \times 10^{-3}$ $((16.2 \pm 0.5) \times 10^{-6})\,M^{-1}\,s^{-1}$, $k_{f,3}$ ($k_{r,3}$): $(0.106 \pm 4) \times 10^{-6}$ $((2.0 \pm 0.2) \times 10^{-6})\,M^{-1}\,s^{-1}$ [62]. In this simultaneous fit the ratios of $k_{f,i}$ and $k_{r,i}$ have been fixed to the equilibrium constants K_i determined after full equilibration.

In the case of complex formation of DMS and acetonitrile with *fac*-$[(CO)_3Tc(H_2O)_3]^+$ ^{99}Tc NMR can be used instead of ^{1}H NMR to follow the replacement of H_2O molecules. Three new signals appear successively in the ^{99}Tc NMR spectrum at −907, −1023 and −1230 ppm (DMS) and −911, −981 and −1098 ppm (CH_3CN) corresponding respectively to the mono, bi, and tri complexes (Fig. 19) [43]. Whereas the signals at −907 and −1023 ppm are relatively broad, the peak at −1230 ppm is again sharp similar to the peak of the triaqua complex at −868 ppm. This is a smart illustration of how the higher symmetry of the "tri complexes" compared to the "bi complexes" affects the quadrupolar relaxation of the ^{99}Tc nucleus leading to slower relaxation rates.

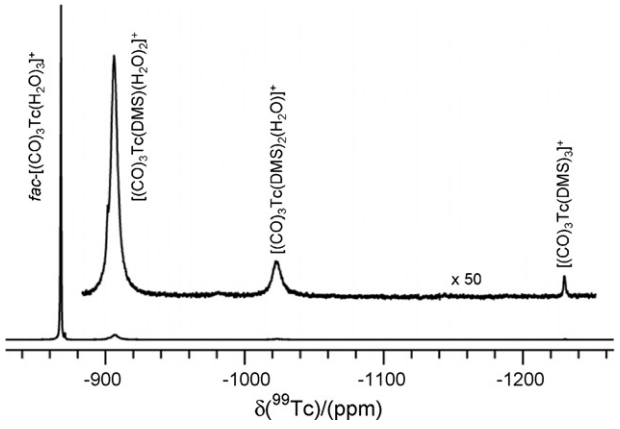

Fig. 19. ^{99}Tc NMR (90 MHz) spectrum of an aqueous solution of *fac*-$[(CO)_3Tc(H_2O)_3]^+$ (31 mM) with dimethylsulfide (22 mM).

The complex formation of DMS with *fac*-$[(CO)_3Mn(H_2O)_3]^+$ is too fast to be studied by looking on the increase with time of peaks in the ^{1}H NMR spectrum. In case of excess of DMS, complexes with one, two and three DMS molecules are formed (Fig. 20) [36]. Increasing temperature leads to broadening of the free and bound DMS signals due to exchange. A study of formation of bi and tri complexes by line broadening of ^{1}H resonance is impossible due to the overlap of the broadened peaks and due to the problem of separation of the broadening effects from different reactions. To study kinetics at variable temperature, ligand concentrations have been chosen so as to have only the mono complex and free ligand in solution ([ligand]/[metal]: 1:50–60, $K_1^{298} = 25.2\,M^{-1}$). Being in the slow exchange domain the half-widths of the ^{1}H NMR peaks are due to magnetic field inhomogeneity, $\Delta\nu^*$, transverse relaxation, $1/T_2$, and residence time, τ_m, at the site corresponding to the peak of the observed nucleus. The transverse relaxation effect is in this case much smaller than the inhomogeneity effect which can be measured on a reference compound present in solution (3-(trimethylsilyl)-1-propane-sulfonic acid, TMSPS). Assuming a second order rate law for the complex formation rate, the residence times of DMS in *fac*-$[(CO)_3Mn(DMS)(H_2O)_2]^+$, τ_{ML}, and as free molecule in solution, τ_L, are linked to the rate constants Eq. (9) [43]:

$$\frac{1}{\tau_L} = k_{f,1}[M] \quad \text{and} \quad \frac{1}{\tau_{ML}} = k_{r,1} \tag{9}$$

Furthermore, the ratio of both residence times is equal to the ratio of the mole fractions, x_L and x_{ML}, of both species in solution Eq. (10):

$$\frac{\tau_{ML}}{\tau_L} = \frac{x_{ML}}{x_L} \quad \text{with} \quad x_L = \frac{[L]}{[ML] + [L]} \quad \text{and}$$
$$x_{ML} = \frac{[ML]}{[ML] + [L]} \tag{10}$$

The equilibrium constant K_1 can be determined from integration of the peaks and independently from the ratio of the rate constants $k_{f,1}/k_{r,1}$ measured from line width. Fig. 21 shows that the results are in agreement. The second order rate constant

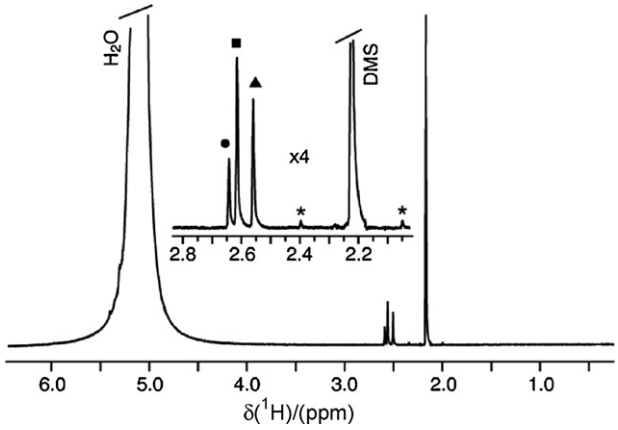

Fig. 20. ^{1}H NMR (400 MHz) spectrum of a *fac*-$[(CO)_3Mn(H_2O)_3]^+$ solution with DMS in excess. *fac*-$[(CO)_3Mn(H_2O)_3^+]$ = 9 mM, [DMS] = 56 mM; (☆) ^{13}C satellites of free DMS.

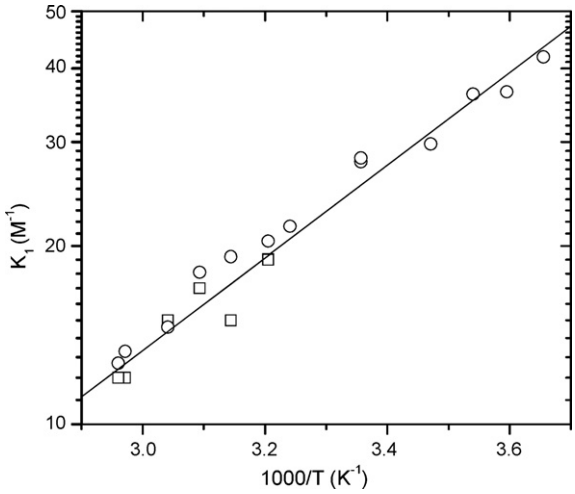

Fig. 21. Temperature dependence of the equilibrium constant K_1 of *fac*-$[(CO)_3Mn(DMS)(H_2O)_2]^+$ from NMR integration (◯) and from the ratio of rate constants $k_{f,1}/k_{r,1}$ (□). $[Mn^I] = 0.048$ M, [DMS] = 0.0017 M, $[H^+] = 0.1$ M.

for formation of *fac*-$[(CO)_3Tc(DMS)(H_2O)_2]^+$ and its temperature dependence are shown in Fig. 22 ($k_{f,1}^{333} = 122 \pm 20\ M^{-1}\ s^{-1}$, $\Delta H^{\ddagger} = 71.2 \pm 12\ kJ\ mol^{-1}$).

Complex formation reactions on group 7 tricarbonyl triaqua complexes have been studied for DMS and CH_3CN and thermodynamic and kinetic data are available (Table 4) [43,46]. For all three metals, complexes are less stable with CH_3CN than with DMS. This difference decreases when going down the group 7, mainly because the stability of the DMS complex decreases. The higher affinity for the S-binding DMS compared to the N-binding CH_3CN is also visible by the slightly faster substitution of water by DMS. The substitution rate by DMS is ∼4 times larger than that by CH_3CN in the case of Mn^I but only 1.5 and 1.2 times larger for Tc^I and Re^I, respectively.

A comparison between the second order complex formation rate constant, $k_{f,1}$, and the water exchange rate constant, k_{ex}, is possible if the Eigen–Wilkins model [63,64] for substitution mechanisms on octahedral complexes is considered. In this

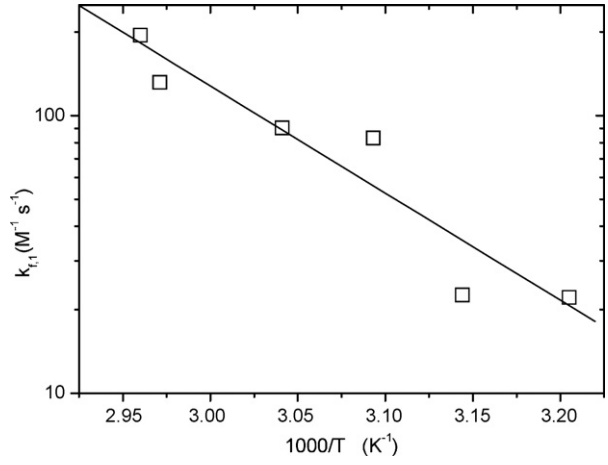

Fig. 22. Temperature dependence of the formation rate constant $k_{f,i}$ of *fac*-$[(CO)_3Mn(DMS)(H_2O)_2]^+$ from NMR line width (□). $[Mn^I] = 0.048$ M, [DMS] = 0.0017 M, $[H^+] = 0.1$ M.

model, it is assumed that the formation of an encounter complex is diffusion controlled and thermodynamically quantified by the equilibrium constant K_{os}. The next step in this reaction scheme consists of the exchange between ligands in the first and the second coordination spheres of the metal and its rate constant, k_i, is rate determining for the whole reaction. The overall rate of the complex formation is therefore $k_f = k_i K_{os}$.

To be able to compare the water exchange rate constant k_{ex} to k_i a statistical factor f/n_c has to be considered [55], where f is the number of molecules in the second coordination sphere and n_c is the number of equivalent water molecules in the first sphere. The rate constants to compare are therefore k_{ex} and k_i' (Eq. (11)):

$$k_i' = \frac{k_f}{K_{os}} \frac{f}{n_c} = \frac{k_f}{K_{os}} \frac{12}{3} \tag{11}$$

whereas the value of $n_c = 3$ is evident in *fac*-$[(CO)_3M(H_2O)_3]^+$ compounds the value for f is less clear and a value of $f = 12$ is generally assumed [55]. The values of K_{os} can be estimated with the Fuoss–Eigen equation [65,66] and typical values are $0.24\ M^{-1}$ for neutral ligands and $1.1\ M^{-1}$ for oppositely charged ligands. As can be seen from the values in Table 5 k_i' and k_{ex} are of the same order of magnitude with at most a factor of 4 difference in the case of DMS.

The most rate and equilibrium constants on complex formation on tricabonyl metal triaqua complexes are available on *fac*-$[(CO)_3Re(H_2O)_3]^+$ [46,62]. A series of N- and S-bonded ligands, neutral and negatively charged ligands have been studied (Table 5). A slight dependence of substitution rates on the chemical nature of incoming ligand is observed. The softer S-bonded ligands have a little faster complex formation than for example the O- and N-bonded ligands, a trend which is even more marked if the interchange rate constants from the Eigen–Wilkins model, k_i', are compared.

An interesting feature of the complex formation of *fac*-$[(CO)_3Re(H_2O)_3]^+$ with the ligands studied is the strong increase in the rate constant for the back reaction, $k_{r,1}$ [62]. From the pyrazine (Pyz) ligand to Br^- it increases by nearly three orders of magnitude (Table 5). This marked leaving group effect represents the changing nucleofugal ability of each species, which is inversely related to their basic character [62]. Bromide with a pK_a (HBr) = −4.7 is the fastest leaving group and Pyz with pK_a (Pyz) = 0.6 is the slowest one. Since $k_{f,1}$ barely changes between ligands the change in equilibrium constant $K_1 = k_{f,1}/k_{r,1}$ originates from the change in $k_{r,1}$. A plot of $\log k_{r,1}$ versus $-\log K_1$ gives a straight line with a slope close to 1 (0.93 ± 0.07) (Fig. 23) [62]. Langford pointed out that a slope of 1 for the straight line indicates that the nature of the leaving group in the transition state is about the same as that in the product, namely a solvated species, one could conclude to a dissociatively activated mechanism for complex formation on *fac*-$[(CO)_3Re(H_2O)_3]^+$. However, because the constant of formation, $k_{f,1}$, is not completely independent on the incoming ligand, L, the complex formation reaction cannot be totally insensitive to the nature of L. To take into account the effect of charge of L the equilibrium constant of the interchange step $K_{1i} = k_i/k_{r,1} = K_1/K_{os}$ could be used in the free

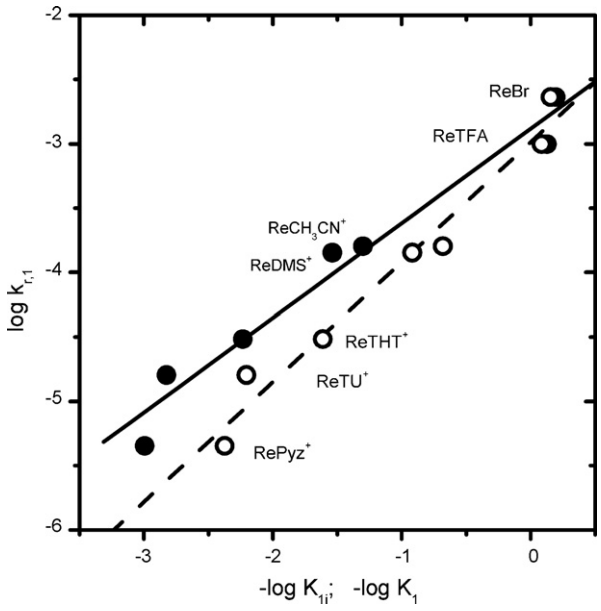

Fig. 23. Plot of the linear regression of $\log k_{r,1}$ versus $-\log K_1$ (◯) with a slope of 0.93 ± 0.07 (– –) and of $\log k_{r,1}$ versus $-\log K_{1i}^{298}$ (●) with a slope of 0.73 ± 0.06 (—) ($T = 298$ K).

energy relationship (Fig. 23). The slope decreases to 0.73 ± 0.06, which is less indicative of a dissociative character of the substitution.

The water exchange rate k_{ex} is close to all interchange rate constants k_i', revealing that the rate of complex formation might be limited by the Re–H_2O bond-breaking. Langford and Gray [67] define an I_d mechanism as the one with greatest influence of the leaving group and an I_a mechanism with the highest sensitivity toward the nature of the entering group. It is therefore difficult to decide on the mechanism only from the rate constants for different ligands. Activation volumes, $\Delta V^{\ddagger}$, measured from pressure dependence of the rate constants, are generally considered as important parameters for corroboration of reaction mechanisms [12,13]: negative $\Delta V^{\ddagger}$ are indicative for an associative activation mode and positive $\Delta V^{\ddagger}$ for a dissociative one. Activation volumes measured range from negative values for the S-bonded ligands DMS and THT ($\Delta V^{\ddagger} = -12$ and $-6.6\,cm^3\,mol^{-1}$, respectively) to a positive value for the N-bonded Pyz ($\Delta V^{\ddagger} = +5.4\,cm^3\,mol^{-1}$) [43,62]. The mechanism of complex formation of *fac*-$[(CO)_3Re(H_2O)_3]^+$ seems to change from I_d, for the harder Pyz, occurring when discrimination between water and entering ligand is poor, to I_a for the softer DMS and THT which are the best nucleophiles (Fig. 24). Activation volumes on complexes of the harder metal centre Mn^I are positive ($\Delta V^{\ddagger} = +4.2$ and $+4.2\,cm^3\,mol^{-1}$ for CH_3CN and DMS, respectively) and clearly indicative for an I_d mechanism to operate.

7. Reactions on *fac*-$[(CO)_2(NO)Re(H_2O)_3]^{2+}$

Besides the tricarbonyl precursors *fac*-$[(CO)_3M(H_2O)_3]^+$ another interesting class of molecules can be obtained by replacing one CO ligand by NO^+ [68–71]. Compared to the

Table 4
Thermodynamic and kinetic parameters for water substitution on *fac*-$[(CO)_3M(H_2O)_3]^+$ complexes (M = Mn, Tc, Re) [43]

L	K_1^{298} (M^{-1})	$\Delta H_{f,1}$ (kJ mol^{-1})	$\Delta S_{f,1}$ (J K^{-1} mol^{-1})	$k_{f,1}^{298}$ (M^{-1} s^{-1})	$k_i'^{298}$ (s^{-1})	$\Delta H_{f,1}^{\ddagger}$ (kJ mol^{-1})	$\Delta S_{f,1}^{\ddagger}$ (kJ mol^{-1})	$\Delta V_{f,1}^{\ddagger}$ (cm^3 mol^{-1})
fac-$[(CO)_3Mn(H_2O)_3]^+$								
CH_3CN	4.5	−13.8	−33.8	1.75	29	83.9	+41.3	+4.2
DMS	25.2	−15.0	−23.3	5.34	89	71.2	+8.1	+11.3
H_2O					23	72.5	+24.4	+7.1
fac-$[(CO)_3Tc(H_2O)_3]^+$								
CH_3CN	2.9	−0.7	+6.5	0.0399	0.665	77.8	−10.0	
DMS	14.9	−6.8	−0.3	0.0608	1.01	70.6	−31.1	
H_2O					0.490	78.3	+11.7	+3.8
fac-$[(CO)_3Re(H_2O)_3]^+$								
Pyz	237			0.00106	0.0177			+5.4
CH_3CN	4.8	−12.3	−28.4	0.00076	0.013	98.6	+26.6	
DMS	8.3			0.00118	0.020			−12
H_2O					0.0054	90.3	+14.5	

Table 5
Rate and equilibrium constants for complex formation of *fac*-$[(CO)_3Re(H_2O)_3]^+$ with various ligands L at $I = 1$ M, $T = 298$ K

	N-bonded [62]		S-bonded [62]			Anionic [46]	
	CH_3CN	Pyz	DMS	THT	TU	CF_3COO^-	Br^-
$10^3\,k_{f,1}$ (M^{-1} s^{-1})	0.76	1.06	1.18	1.28	2.49	0.81	1.6
$10^5\,k_{r,1}$ (s^{-1})	16	0.45	14.2	3.05	1.6	99	230
$10^3\,k_i'$ (s^{-1})[a]	12.7	17.7	20	21	41.5	2.9	5.8
K_1 (M^{-1})	4.8	237	8.3	41	160	0.82	0.7

[a] Water exchange rate $k_{ex} = 6.3 \times 10^{-3}$ s^{-1}.

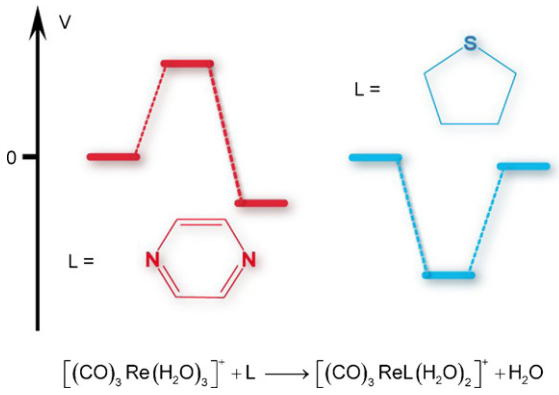

Fig. 24. Water substitution by Pyz (left) and THT (right) on *fac*-$[(CO)_3Re(H_2O)_3]^+$: volume profiles showing change in reaction mechanism from I_d (Pyz) to I_a (THT).

fac-$[(CO)_3M]^+$ the presence of the NO^+ ligand increases the positive charge of the complex to 2+. Furthermore, the nitrosyl ligand is considered to have a lower σ-donor and higher π-acceptor strength than the carbonyl ligand [72]. These factors increase the hardness of *fac*-$[(CO)_2(NO)M]^+$ compared to *fac*-$[(CO)_3M]^+$ and thus, a preference for different chelating ligands may result.

7.1. Water exchange on *fac*-$[(CO)_2(NO)Re(H_2O)_3]^{2+}$

Replacement of one CO by a NO^+ makes the three more labile coordination sites on *fac*-$[(CO)_2(NO)M]^+$ different. One consequence is that bound water molecules are no longer equivalent and exchange rates from water *cis* and *trans* to the nitroxyl are different. The ^{17}O NMR spectrum of an isotopically equilibrated solution of *fac*-$[(CO)_2(NO)Re(H_2O)_3]^+$ in 3% enriched $H_2{}^{17}O$ shows three signals at 389, −6 and −32 ppm with integral ratios 2:1:2 (Fig. 25) [72]. The peaks were assigned to two CO ligands, one H_2O *trans* to NO and two H_2O *cis* to NO. The signal of bulk water disappeared due to addition of strongly paramagnetic Mn^{2+}. No signal due to NO-oxygen could be detected with and without Mn^{2+} probably due to extremely slow oxygen exchange on nitrosyl even in acidic solution [72].

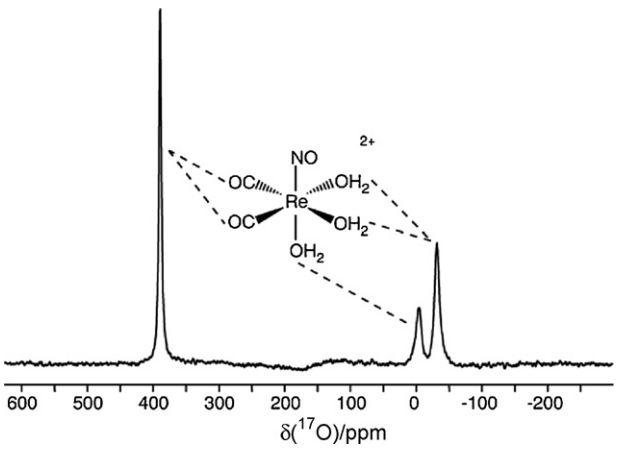

Fig. 25. ^{17}O NMR spectrum of a solution of *fac*-$[(CO)_2(NO)Re(H_2O)_3]^{2+}$ in CF_3SO_3H 1 M after addition of ^{17}O-enriched water (3%) in the presence of Mn^{2+} (0.1 M).

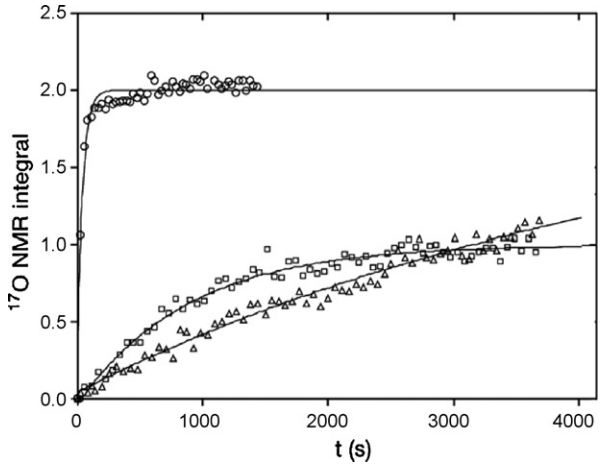

Fig. 26. Increase of ^{17}O NMR signal integrals as a function of time at $T = 298$ K and $[H^+] = 1$ M on a solution of $[(CO)_2(NO)Re(H_2O)_3]^{2+}$: (◯) CO ligand, (□) H_2O-*trans* NO, (△) H_2O-*cis* NO.

Water exchange on *cis* and *trans* position is slow and could be followed by isotopic enrichment. After injection of water 20% enriched in ^{17}O into a solution of *fac*-$[(CO)_2(NO)Re(H_2O)_3]^{2+}$ containing Mn^{2+} the increase in signal intensities of bound water and CO has been monitored as a function of time (Fig. 26). Clearly, the exchange of the water molecule *trans* to NO is faster than the two water molecules *cis* to NO. Under the experimental conditions given in Fig. 26 the observed exchange rate constants are $k_{obs}^{trans} = 1.13 \times 10^{-3}\ s^{-1}$ and $k_{obs}^{cis} = 0.209 \times 10^{-3}\ s^{-1}$.

Studying the exchange rates as a function of $[H^+]$, a strongly non-linear dependence of both k_{obs}^{trans} and k_{obs}^{cis} as a function of $[H^+]$ has been found (Fig. 27). The observed rate constants $k_{obs}^{trans/cis}$ can be calculated from the water exchange rate constants on *fac*-$[(CO)_2(NO)Re(H_2O)_3]^{2+}$ ($k_{ex}^{trans/cis}$) and on

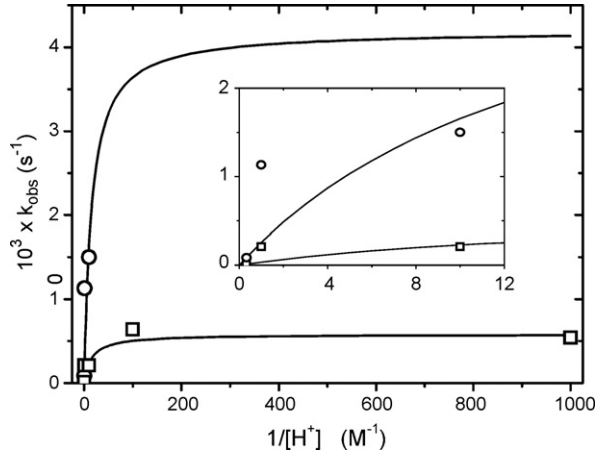

Fig. 27. Observed rate constants k_{obs}^{trans} (◯) and k_{obs}^{cis} (□) for water exchange reactions in *trans* and *cis* positions to the NO ligands in *fac*-$[(CO)_2(NO)Re(H_2O)_3]^{2+}$ as a function of acidity ($T = 298$ K).

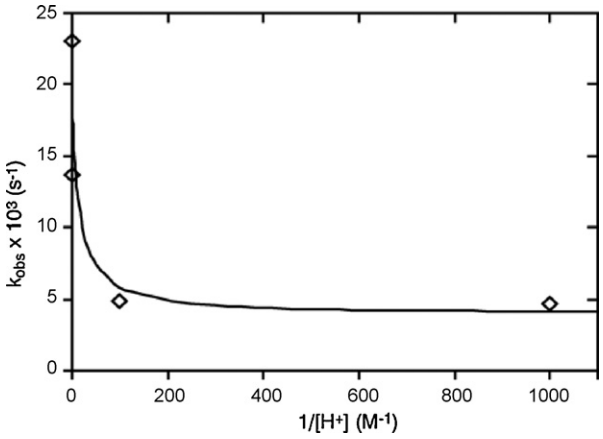

Fig. 28. Observed rate constants $k_{obs}^{C^*O}$ for oxygen exchange between ^{17}O enriched water and the carbonyl oxygen on *fac*-$[(CO)_2(NO)Re(H_2O)_3]^{2+}$ as a function of acidity ($T = 298.0$ K).

fac-$[(CO)_2(NO)Re(OH)(H_2O)_2]^+$ ($k_{OH}^{trans/cis}$) as Eq. (12):

$$k_{obs}^{trans/cis} = x_{Re}k_{ex}^{trans/cis} + x_{ReOH}k_{OH}^{trans/cis} \quad \text{with}$$

$$x_{Re} = \frac{[H^+]}{[H^+] + K_a} \quad \text{and} \quad x_{ReOH} = \frac{K_a}{[H^+] + K_a} \qquad (12)$$

Analysis of the experimental $k_{obs}^{trans/cis}$ shows that exchange of *trans* and *cis* water of the non-hydrolyzed species is very slow compared to exchange on the hydrolyzed complex and $k_{obs}^{trans/cis} \simeq x_{ReOH}k_{OH}^{trans/cis}$. Exchange rate constants determined on *fac*-$[(CO)_2(NO)Re(OH)(H_2O)_2]^+$ are $k_{OH}^{trans} = 4.2 \times 10^{-3}\ s^{-1}$ and $k_{OH}^{cis} = 0.58 \times 10^{-3}\ s^{-1}$ [72]. Both exchange rates are several orders of magnitude slower than water exchange rates on *fac*-$[(CO)_3Re(OH)(H_2O)_2]$ ($k_{OH} = 27\ s^{-1}$). However, the hydrolyzed complex *fac*-$[(CO)_2(NO)Re(OH)(H_2O)_2]^+$ and *fac*-$[(CO)_3Re(H_2O)_3]^+$ have the same charge and their water exchange rates are of the same order of magnitude. The fact that the ^{17}O NMR signal of the *trans* water molecule is strongly broadened as the acidity is decreased suggests that deprotonation occurs on the water *trans* to the nitroxyl. The pK_a value determined from the data analysis is $\sim 1.2 \pm 0.2$ showing that *fac*-$[(CO)_2(NO)Re(H_2O)_3]^{2+}$ is much more acidic than *fac*-$[(CO)_3Re(H_2O)_3]^+$ ($pK_a = 7.5$) [47]. The value calculated from the acidity dependence of k_{obs} is lower than the pK_a calculated from the acidity of a 1 mM solution of the complex ($pK_a = 2.96$) [69].

From Fig. 26 it can be seen that oxygen enrichment on CO is faster than water exchange on *fac*-$[(CO)_2(NO)Re(H_2O)_3]^{2+}$. The acid dependence of $k_{obs}^{C^*O}$ has been analyzed with equations similar to Eq. (5) (Fig. 28). Fixing K_a to the value determined from the water exchange ($pK_a = 1.2$), exchange rate constants for oxygen exchange on *fac*-$[(CO)_2(NO)Re(H_2O)_3]^{2+}$ and on *fac*-$[(CO)_3Re(OH)(H_2O)_2]^+$ have been determined to $k_{Re}^{C^*O} = (19 \pm 4) \times 10^{-3}\ s^{-1}$ and $k_{ReOH}^{C^*O} = (4 \pm 3) \times 10^{-3}\ s^{-1}$, respectively. Such oxygen enrichment on CO has not been observed for *fac*-$[(CO)_3Re(H_2O)_3]^+$ in acidic solution [46] but has been reported for *fac*-$[(CO)_3Mn(H_2O)_3]^+$ [43,61] and $[(CO)_nRu(H_2O)_{6-n}]^+$ [37].

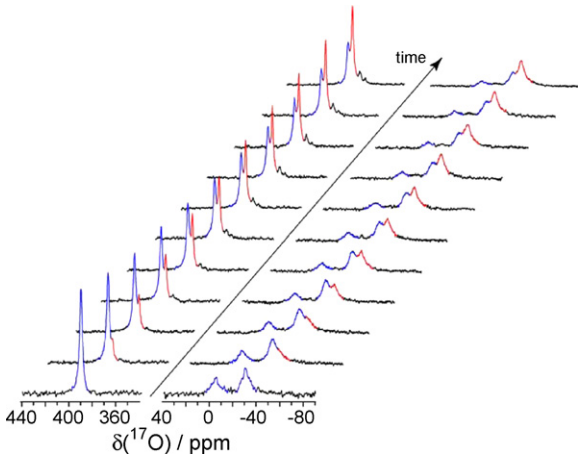

Fig. 29. Increase of ^{17}O NMR signal integrals as a function of time at $T = 298.0$ K and $[H^+] = 1$ M on a solution of *fac*-$[(CO)_2(NO)Re(H_2O)_3]^{2+}$: (◯) CO ligand, (□) H_2O-*trans* NO, (△) H_2O-*cis* NO.

7.2. Complex formation on *fac*-$[(CO)_2(NO)Re(H_2O)_3]^{2+}$

The triaqua complex *fac*-$[(CO)_2(NO)Re(H_2O)_3]^{2+}$ has been prepared from the bromo complex *fac*-$[(CO)_2(NO)ReBr_3][NEt_4]$ in aqueous solution [72] by adding $AgCF_3SO_3$. To study complex formation of *fac*-$[(CO)_2(NO)Re(H_2O)_3]^{2+}$ with Br^- four equivalents of NaBr have been added to the complex equilibrated in 3% ^{17}O enriched water (1 M [H^+], Mn^{2+}). The reaction was followed for 14 days at 298 K by ^{17}O NMR [36]. Two new signals of about 1:1 ratio started to rise within 10 h after mixing (Fig. 29, red). The water molecule *trans* to NO being the most labile and therefore the first to be replaced, the new signals have been assigned to $[(CO)_2(NO)Re(Br\text{-}trans)(H_2O\text{-}cis)_2]^+$. Further signals start to grow with time and after 14 d seven signals in the carbonyl region (~380 ppm) and 5 signals for coordinated water (~−40 ppm) can be distinguished (Fig. 30). Considering the six possible mono, bi and tri bromide species (including all possible isomers) at most eight CO and seven H_2O signals can be expected in the ^{17}O NMR spectrum (free water being

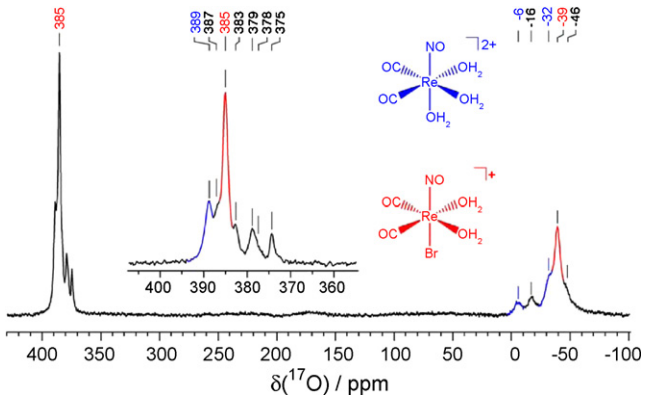

Fig. 30. ^{17}O NMR spectrum of a solution with 0.05 M *fac*-$[(CO)_2(NO)Re(H_2O)_3]^{2+}$ in 3% ^{17}O-enriched water recorded 14 days after addition of 4 equivalents of NaBr ($[H^+] = 1$ M, Mn^{2+} present for free water suppression). Resolution enhancement has been applied to the extended part of the CO region.

suppressed by Mn^{2+}). The spectrum recorded (Fig. 30) shows that nearly all possible complexes have been formed after 14 d.

8. Concluding remarks

The first concern of this review was to present several experimental NMR techniques to study ligand exchange and complex formation reactions of *fac*-$[(CO)_3M(H_2O)_3]^+$ (M = Mn, Tc, Re) and on *fac*-$[(CO)_2(NO)Re(H_2O)_3]^{2+}$. It has been shown that sometimes combinations of techniques applied at variable temperature or variable pressure allowed to measure exchange rate constants and their activation parameters as well as thermodynamic parameters. Furthermore, the uses of uncommon nuclei for NMR like ^{17}O or ^{99}Tc extends considerably the range of applications especially in aqueous solutions when ^{1}H NMR is often not very useful.

The second concern of this paper is to give a short overview on kinetic studies performed on tricarbonyl triaqua complexes of technetium(I) and rhenium(I) which became precursors for a variety of radiopharmaceuticals under development. It has been shown that the *fac*-$[(CO)_3M]$ unit is kinetically inert and that water molecules bound to it can be replaced easily. Reactivity of the Re^I complexes is one to two orders of magnitude slower than its Tc^I analogues. Furthermore, it shows a marked acidity dependence which has not been observed for Tc^I and Mn^I species.

Acknowledgements

The author is indebted to Andre Merbach, who supervised most of the work presented, for very stimulating discussions during many years. The Swiss National Science Foundation is gratefully acknowledged for financial support.

References

[1] H.S. Gutowsky, A. Saika, J. Chem. Phys. 21 (1953) 1688.
[2] H.S. Gutowsky, C.H. Holm, J. Chem. Phys. 25 (1956) 1228.
[3] H.S. Gutowsky, R.L. Vold, E.J. Wells, J. Chem. Phys. 43 (1965) 4107.
[4] H.M. McConnell, J. Chem. Phys. 28 (1958) 430.
[5] L.M. Jackman, F.A. Cotton (Eds.), Dynamic Nuclear Magnetic Resonance Spectroscopy, Academic, New York, NY, 1975.
[6] J.I. Kaplan, G. Fraenkel, NMR of Chemically Exchanging Systems, Academic Press, New York, NY, 1980.
[7] J. Sandström, Dynamic NMR Spectroscopy, Academic Press, London, UK, 1982.
[8] M.L. Martin, G.J. Martin, J. Delpuech, Practical NMR Spectroscopy, Heyden, London, UK, 1980.
[9] G. Binsch, H. Kessler, Angew. Chem., Int. Ed. 19 (1980) 411.
[10] A.D. Bain, Prog. NMR Spectrosc. 43 (2003) 63.
[11] A.D. Bain, G.J. Duns, in: G. Batta, K. Kövér, J. Scántay (Eds.), Methods for Structure Elucidation by High-Resolution NMR, vol. 8, Elsevier, Amsterdam, The Netherlands, 1997, p. 357.
[12] L. Helm, G.M. Nicolle, A.E. Merbach, Adv. Inorg. Chem. 57 (2005) 327.
[13] F.A. Dunand, L. Helm, A.E. Merbach, Adv. Inorg. Chem. 54 (2003) 1.
[14] L. Helm, A.E. Merbach, Chem. Rev. 105 (2005) 1923.
[15] K. Schwochau, Technetium: Chem. Radiopharm. Appl., Wiley-VCH, Weinheim, Germany, 2000.
[16] K. Schwochau, Angew. Chem., Int. Ed. 33 (2003) 2258.
[17] D.S. Urch, M.J. Welch, Ann. Rep. Prog. Chem., Sect. A 101 (2005) 585.
[18] D.S. Urch, M.J. Welch, Ann. Rep. Prog. Chem., Sect. A 102 (2006) 542.
[19] F. Tisato, M. Porchia, C. Bolzati, F. Refosco, A. Vittadini, Coord. Chem. Rev. 250 (2006) 2034.
[20] R. Alberto, R. Schibli, R. Waibel, U. Abram, A.P. Schubiger, Coord. Chem. Rev. 192 (1999) 901.
[21] R. Alberto, U. Abram, in: F. Rösch (Ed.), Handbook of Nuclear Chemistry, vol. 4, Kluwer Academic Publications, Amsterdam, The Netherlands, 2003, p. 211.
[22] R. Alberto, in: J.A. McCleverty, T.J. Meyer (Eds.), Comprehensive Coordination Chemistry II, vol. 5, Elsevier, 2004, p. 127.
[23] R. Alberto, in: W. Krause (Ed.), Topics in Current Chemistry, vol. 252, Springer, Berlin, Germany, 2005, p. 1.
[24] E. Garcia-Garayoa, R. Schibli, P.A. Schubiger, Nucl. Sci. Tech. 18 (2007) 88.
[25] N.J. Stone, At. Data Nucl. Data Tables 90 (2005) 75.
[26] U. Abram, R. Alberto, J. Braz. Chem. Soc. 17 (2006) 1486.
[27] R. Alberto, J. Organomet. Chem. 692 (2007) 1179.
[28] R. Alberto, R. Schibli, A. Egli, P.A. Schubiger, W.A. Herrmann, G. Artus, U. Abram, T.A. Kaden, J. Organomet. Chem. 493 (1995) 119.
[29] R. Alberto, J. Nucl. Radiochem. Sci. 6 (2005) 173.
[30] S.R. Banerjee, P. Schaffer, J.W. Babich, J.F. Valliant, J. Zubieta, Dalton Trans. (2005) 3886.
[31] M. Allali, S. Cousinie, M. Gressier, C. Tessier, A.L. Beauchamp, Y. Coulais, M. Dartiguenave, E. Benoist, Inorg. Chim. Acta 359 (2006) 2128.
[32] C.L. Ferreira, S.R. Bayly, D.E. Green, T. Storr, C.A. Barta, J. Steele, M.J. Adam, C. Orvig, Bioconjug. Chem. 17 (2006) 1321.
[33] L. Maria, A. Paulo, I.C. Santos, I. Santos, P. Kurz, B. Spingler, R. Alberto, J. Am. Chem. Soc. 128 (2006) 14590.
[34] L. Maria, S. Cunha, M. Videira, L. Gano, A. Paulo, I.C. Santos, I. Santos, Dalton Trans. (2007) 3010.
[35] M. McFarlane, H.C.E. McFarlane, in: J. Mason (Ed.), Multinuclear NMR, Plenum Press, New York, USA, 1987, p. 403.
[36] P. Grundler, Ph.D. Thesis, Ecole Polytechnique Fédérale de Lausanne, Lausanne, Switzerland, 2005.
[37] U.C. Meier, R. Scopelliti, E. Solari, A.E. Merbach, Inorg. Chem. 39 (2000) 3816.
[38] P.J. Hore, J. Magn. Reson. 55 (1983) 283.
[39] P.J. Hore, J. Magn. Reson. 54 (1983) 539.
[40] Y. Ducommun, K.E. Newman, A.E. Merbach, Inorg. Chem. 19 (1980) 3696.
[41] D. Hugi Cleary, L. Helm, A.E. Merbach, J. Am. Chem. Soc. 109 (1987) 4444.
[42] S.F. Lincoln, A.E. Merbach, Adv. Inorg. Chem. 42 (1995) 1.
[43] P.V. Grundler, L. Helm, R. Alberto, A.E. Merbach, Inorg. Chem. 45 (2006) 10378.
[44] P. Bernhard, L. Helm, A. Ludi, A.E. Merbach, J. Am. Chem. Soc. 107 (1985) 312.
[45] A. Abragam, The Principles of Nuclear Magnetism, Clarendon Press, Oxford, UK, 1961.
[46] B. Salignac, P.V. Grundler, S. Cayemittes, U. Frey, R. Scopelliti, A.E. Merbach, R. Hedinger, K. Hegetschweiler, R. Alberto, U. Prinz, G. Raabe, U. Koelle, S. Hall, Inorg. Chem. 42 (2003) 3516.
[47] A. Egli, K. Hegetschweiler, R. Alberto, U. Abram, R. Schibli, R. Hedinger, V. Gramlich, R. Kissner, A.P. Schubiger, Organometallics 16 (1997) 1833.
[48] G. Laurenczy, I. Rapaport, D. Zbinden, A.E. Merbach, Magn. Reson. Chem. (1991) S45.
[49] I. Rapaport, L. Helm, A.E. Merbach, P. Bernhard, A. Ludi, Inorg. Chem. 27 (1988) 873.
[50] D. De Vito, E. Sidorenkova, F.P. Rotzinger, J. Weber, A.E. Merbach, Inorg. Chem. 39 (2000) 5547.
[51] U. Prinz, Ph.D. Thesis, RWTH Aachen, Aachen, Germany, 2000.
[52] A. Cusanelli, U. Frey, D.T. Richens, A.E. Merbach, J. Am. Chem. Soc. 118 (1996) 5265.
[53] A. Cusanelli, U. Frey, D. Marek, A.E. Merbach, Spectrosc. Europe 9 (1997) 22.
[54] N. Aebischer, R. Schibli, R. Alberto, A.E. Merbach, Angew. Chem., Int. Ed. 39 (2000) 254.
[55] N. Aebischer, R. Churlaud, L. Dolci, U. Frey, A.E. Merbach, Inorg. Chem. 37 (1998) 5915.

[56] A.W. Ehlers, Y. Ruiz-Morales, E.J. Baerends, T. Ziegler, Inorg. Chem. 36 (1997) 5031.
[57] J. Kowalewski, L. Mäler, Nuclear Spin Relaxation in Liquids: Theory, Experiments, and Applications, Taylor & Francis, New York, USA, 2006.
[58] R. Alberto, R. Motterlini, Dalton Trans. (2007) 1651.
[59] E.L. Muetterties, Inorg. Chem. 4 (1966) 1841.
[60] D.J. Darensbourg, J.A. Froelich, J. Am. Chem. Soc. 99 (1977) 4726.
[61] U. Prinz, U. Koelle, S. Ulrich, A.E. Merbach, O. Maas, K. Hegetschweiler, Inorg. Chem. 43 (2004) 2387.
[62] P.V. Grundler, B. Salignac, S. Cayemittes, R. Alberto, A.E. Merbach, Inorg. Chem. 43 (2004) 865.
[63] M. Eigen, K. Tamm, Z. Elektrochem. 66 (1962) 93.
[64] M. Eigen, R.G. Wilkins, Adv. Chem. Ser. 49 (1965) 55.
[65] R.M. Fuoss, J. Am. Chem. Soc. 80 (1958) 5050.
[66] M. Eigen, W. Kruse, G. Maass, L. de Maeyer, Prog. React. Kinet. 2 (1964) 285.
[67] C.H. Langford, H.B. Gray, Ligand Substitution Processes, W.A. Benjamin Inc., New York, USA, 1965.
[68] D. Rattat, A. Verbruggen, H. Berke, R. Alberto, J. Organomet. Chem. 689 (2004) 4833.
[69] D. Rattat, A. Verbruggen, H. Schmalle, H. Berke, R. Alberto, Tetrahedron Lett. 45 (2004) 4089.
[70] R. Schibli, N. Marti, P. Maurer, B. Spingler, M.-L. Lehaire, V. Gramlich, C.L. Barnes, Inorg. Chem. 44 (2005) 683.
[71] P. Kurz, D. Rattat, D. Angst, H. Schmalle, B. Spingler, R. Alberto, H. Berke, W. Beck, Dalton Trans. (2005) 804.
[72] M.-L. Lehaire, P.V. Grundler, S. Steinhauser, N. Marti, L. Helm, K. Hegetschweiler, R. Schibli, A.E. Merbach, Inorg. Chem. 45 (2006) 4199.